

The efficacy of exosomes from human chemically derived hepatic progenitors in liver damage alleviation: a preclinical experimental study

Min Kim^{1,2,3}, Tae Hun Kim^{1,2,3}, Elsy Soraya Silva Salas^{1,2,3}, Soyoung Jeon^{1,2,3}, Ji Hyun Shin^{1,2,3}, Dongho Choi^{1,2,3}

¹Department of Surgery, Hanyang University College of Medicine, Seoul, Korea

²Research Institute of Regenerative Medicine and Stem Cells, Hanyang University, Seoul, Korea

³Hanyang Institute of Bioscience and Biotechnology, Hanyang University, Seoul, Korea

Purpose: Over the past decade, interest in exosomes as therapeutics has surged. In particular, stem-cell-derived exosomes may be more effective as a treatment for liver disease than the stem cells themselves. We have previously developed human chemically derived hepatic progenitors (hCdHs) from human hepatocytes. hCdHs can differentiate into hepatocytes and cholangiocytes, regenerating the liver in mouse models. In this study, we evaluated the mitigating effects of hCdHs-derived exosomes (hCdHs-exo) on liver damage and compared them with those of exosomes from bone marrow mesenchymal stem cells (BMMSCs-exo).

Methods: Exosomes were isolated from hCdHs and BMMSCs by culturing cells in large quantities and separating the exosomes from the culture medium using ultracentrifugation. Isolated exosomes were characterized by various methods before experimental use. *In vitro*, the ability of exosomes to inhibit activation of hepatic stellate cells (HSCs) by transforming growth factor beta 1 was evaluated. *In vivo*, exosomes were injected into mice with carbon tetrachloride (CCl₄)-induced liver damage, and their effectiveness in mitigating liver damage was assessed by histological staining and biochemical analysis.

Results: The analyses confirmed the successful isolation of exosomes from both cell types. *In vitro*, hCdHs-exo significantly reduced the levels of transcription factors and activation markers in induced HSCs. *In vivo*, hCdHs-exo effectively alleviated liver damage caused by CCl₄. Furthermore, both *in vitro* and *in vivo* studies confirmed that hCdHs-exo had a greater effect in alleviating liver damage than did BMMSCs-exo.

Conclusion: These results demonstrate that hCdHs-exo, similarly to hCdHs, have superior efficacy in alleviating liver damage compared with BMMSCs-exo.

[Ann Surg Treat Res 2024;107(5):252-263]

Key Words: Exosomes, Hepatocytes, Human chemically derived hepatic progenitors, Liver, Mesenchymal stem cells

INTRODUCTION

Exosomes are very small vesicles secreted by cells [1]. In

general, these vesicles play an important role in transmitting information between various cells [2]. Exosomes are produced intracellularly from the plasma membrane before being secreted

Received June 11, 2024, Revised July 22, 2024, Accepted August 18, 2024

Corresponding Author: Dongho Choi

Department of Surgery, Hanyang University College of Medicine, 222 Wangsimni-ro, Seongdong-gu, Seoul 04763, Korea, **Tel:** +82-2-2220-0647, **Fax:** +82-2-2281-0224, **E-mail:** crane87@hanyang.ac.kr, **ORCID:** <https://orcid.org/0000-0002-1255-1964>

Co-Corresponding Author: Ji Hyun Shin

Department of Surgery, Hanyang University College of Medicine, 222 Wangsimni-ro, Seongdong-gu, Seoul 04763, Korea
Tel: +82-2-2220-0647, **Fax:** +82-2-2281-0224, **E-mail:** jhshin0509@hanyang.ac.kr, **ORCID:** <https://orcid.org/0000-0002-1897-7990>

Copyright © 2024, the Korean Surgical Society

© Annals of Surgical Treatment and Research is an Open Access Journal. All articles are distributed under the terms of the Creative Commons Attribution Non-Commercial License (<http://creativecommons.org/licenses/by-nc/4.0/>) which permits unrestricted non-commercial use, distribution, and reproduction in any medium, provided the original work is properly cited.

[3]. Exosomes contain various molecules, such as proteins, RNA, and DNA fragments, that affect the function or behavior of the recipient cells [4]. Owing to these characteristics, exosomes play an essential role in intercellular communication and have been implicated in the development and progression of various diseases, including cancer, cardiovascular disease, and neurologic disorders [5]. Recent research has significantly focused on the potential of using exosomes in disease diagnosis and treatment [6]. For instance, analyzing the components of exosomes secreted in specific disease states could facilitate early diagnosis or assessment of disease progression [7]. Moreover, the development of exosome-based drug delivery systems is currently underway [8].

Before research into potential therapeutic utility of exosomes began, the initial focus was on therapies using stem cells [9]. Stem cell therapy utilizes the regenerative ability of stem cells for the purpose of treating damaged tissues or organs to restore their function [10]. Stem cells are able to differentiate into various cell types, which can be used to treat various diseases [11]. Stem cell therapy remains a developing field, with much research still ongoing [12]. Although the potential offered by this treatment is substantial, it is important to ensure its safety, as side effects such as cancer can occur because of indiscriminate proliferation and differentiation after stem cell transplantation [13].

As an alternative to stem cell transplantation, using exosomes isolated from stem cells to treat damage in different organs has recently attracted attention in medical research [14]. Exosomes derived from stem cells promote tissue regeneration and repair, likely via various growth factors and proteins that they contain [15,16]. Using exosomes obtained from one's own cells reduces the risk of transplant rejection and other complications, including cancer [17].

Exosomes have also been applied as a treatment for various liver diseases, such as fibrosis, hepatitis, and cirrhosis [18]. In liver treatment research, exosomes are primarily isolated from mesenchymal stem cells (MSCs), such as bone marrow MSCs (BMMSCs), adipose-derived MSCs, and umbilical cord MSCs [19].

However, we used liver stem cells known as human chemically derived hepatic progenitors (hCdHs) to isolate exosomes. hCdHs are obtained by treating primary hepatocytes with 3 compounds, hepatocyte growth factor (HGF), A83-01, and CHIR99021, and have the ability to differentiate into hepatocytes and cholangiocytes [20]. These stem cells are an effective treatment that can alleviate liver damage when injected into liver disease model mice [20]. Various studies, including studies of gene editing, organoid formation, and drug screening, have been conducted using hCdHs [21-23]. However, the efficacy of exosomes derived from hCdHs in disease treatment has not yet been explored.

In this study, we sought to isolate and characterize exosomes from liver stem cells, hCdHs, and determine whether these

exosomes have a liver damage-alleviating effect like hCdHs. Additionally, we aimed to compare the efficacy of liver damage alleviation between exosomes derived from MSCs, which have been primarily studied, and those from hCdHs through both *in vitro* and *in vivo* experiments.

METHODS

Ethics statements

The study was performed according to protocols approved by the Institutional Review Board of Hanyang University, Seoul, Korea (No. HYI-16-229-3). Human liver tissues were obtained from the donors with informed consent. The animal experiments were performed with the approval of the Institutional Animal Care and Use Committee (IACUC) of Hanyang University (No. 2023-0242A) and in compliance with the U.S. National Institutes of Health guidelines and the Hanyang University animal research protocol.

Generation of human chemically derived hepatic progenitors

Human liver tissues were obtained from 3 donors undergoing surgery at the Hanyang University Medical Center (Supplementary Table 1). The generation of hCdHs followed a previously published method [20]. In brief, primary hepatocytes were isolated using a modified 2-step collagenase perfusion method. Isolated hepatocytes were seeded on collagen-coated dishes (STEMCELL Technologies) in William's E media (Gibco). The next day, the medium was changed to DMEM/F-12 (Gibco) reprogramming medium containing 4 μ M A83-01 (Gibco), 3 μ M CHIR99021 (STEMCELL Technologies), and 20 ng/mL HGF (Peprotech). The reprogramming medium was changed every 2 days. The hCdHs were generated within 1 week and considered as passage 1.

Isolation of exosomes from human chemically derived hepatic progenitors and bone marrow mesenchymal stem cells

Cells were cultured until they reached 70%–80% confluency and then incubated at 37 °C and 5% CO₂ for 2 days in medium with 10% extracellular vesicles-depleted fetal bovine serum (EV-depleted FBS). The culture supernatant was collected and subjected to several centrifugations for exosome separation. First, the culture supernatant was centrifuged at 300×g for 10 minutes to remove cell debris. Then, the supernatant was clarified by centrifugation at 2,000×g for 10 minutes. Finally, ultracentrifugation was performed at 100,000×g for 70 minutes at 4 °C in a type Ti100 rotor on an XL-100K ultracentrifuge (Beckman) to isolate exosomes. After resuspension in phosphate-buffered saline (PBS), the exosome pellet was ultracentrifuged again for 70 minutes at 100,000×g. The washed exosome pellet was resuspended in filtered (pore size, 0.22 μ m) PBS and stored

at -80°C .

Nanoparticle tracking analysis

Nanoparticle tracking analysis (NTA) was conducted to track automatically the Brownian motion and size distribution of exosomes in real time on a NanoSight LM10 system (Malvern Panalytical). Samples were injected into the chamber and visualized with a 405-nm laser. The recorded images were analyzed using NanoSight NTA 3.2 software (Malvern Panalytical).

Cryo-transmission electron microscopy

The morphology and structure of the exosomes were evaluated using cryogenic transmission electron microscopy (Cryo-TEM). A sample containing 5×10^8 exosomal particles was loaded onto a lacey carbon grid (EMS). The grid was observed with a Tecnai F20 G2 microscope (FEI) at 200 kV.

In vitro exosome uptake assay

To analyze the uptake capacity of exosomes, exosomes were labeled with a lipophilic near-infrared indotricarbocyanine iodide dye (DiR, Invitrogen) for 1 hour at room temperature, after which the free dye was removed by ultracentrifugation through an iodixanol density gradient (OptiPrep, Axis-Shield) at $100,000\times g$ for 18 hours. The purified stained exosomes were added to human hepatic stellate cells (HHStECs) for 4 hours. Nuclei were stained with Hoechst 33342 (1:1,000 dilution, Molecular Probes). Images of exosomes and HHStECs were obtained with an LSM900 live cell imaging system (Zeiss).

Activation of human hepatic stellate cells and treatment with exosomes

HHStECs were purchased from ScienCell and cultured. Transforming growth factor beta 1 (TGF- β 1, 2 ng/mL; R&D Systems) was added to induce HHStEC activation. Simultaneously, the cells were treated with 150- $\mu\text{g}/\text{mL}$ exosomes. The same volume of PBS was added to the control group. The cells were examined after 48-hour incubation.

Quantitative real-time PCR

TRIzol reagents (Invitrogen) were used to isolate total RNA from primary hepatocytes, cultured hCdhHs and HHStECs treated TGF- β 1 and exosomes. RNA was quantified with a NanoDrop spectrophotometer (Thermo Fisher Scientific). Real-time PCR was performed on a CFX Connect Real-Time System (Bio-Rad). A total of 40 2-step cycles (95°C for 20 seconds and 60°C for 40 seconds) were used for PCR amplification. Glyceraldehyde-3-phosphate dehydrogenase (*GAPDH*) was used as the control to evaluate the relative quantitative of messenger RNAs. The $2^{-\Delta\Delta\text{Ct}}$ method was used to calculate the relative expression. The primers are shown in Supplementary Table 2.

Western blot analysis

The protein concentration of the purified exosomes was quantified using a bicinchoninic acid protein assay kit (Thermo Scientific), and the Bradford protein assay method was employed to measure the protein concentration in the cell lysate. Cell lysates and exosomes (10 μg of total protein) were resolved on sodium dodecyl sulfate-polyacrylamide gel electrophoresis (SDS-PAGE) gels and transferred onto polyvinylidene fluoride (PVDF) membranes (Millipore). The membrane was blocked and incubated with primary antibody: (i) exosomal markers: anti-CD9 (1:1,000 dilution, Santa Cruz Biotechnology), anti-CD63 (1:1,000 dilution, Santa Cruz Biotechnology), and anti-CD81 (1:1,000 dilution, Santa Cruz Biotechnology); (ii) non-exosomal markers: anti-GM130 (1:1,000 dilution, Thermo Scientific) and anti-calnexin (1:1,000 dilution, Santa Cruz Biotechnology); (iii) fibrosis markers: anti-alpha smooth muscle actin (α -SMA) (1:1,000 dilution, Abcam) and anti-Col1 (1:1,000 dilution, Abcam). GAPDH (1:5,000 dilution, Abcam) was used for relative protein quantitation. The membranes were incubated with primary antibodies overnight at 4°C and washed with tris-buffered saline with Tween 20 (TBST). The membranes were then incubated with secondary antibodies (goat anti-mouse immunoglobulin G [IgG], goat anti-rabbit IgG; 1:5,000 dilution; GeneTex) for 1 hour at room temperature and washed again with TBST. The immunoreactive bands were visualized using WestGlow FEMTO Chemiluminescent Substrate (Biomax).

Immunofluorescence staining

Primary hepatocytes, cultured hCdhHs, and HHStECs were fixed in 4% paraformaldehyde (PFA) for 20 minutes at room temperature. The fixed cells were washed with PBS and blocked with 1% bovine serum albumin (BSA) and 10% sodium azide. The cells were incubated with anti-AFP (1:100 dilution, R&D Systems), anti-EpCAM (1:100 dilution, Abcam), anti-CK19 (1:100 dilution, Santa Cruz Biotechnology), anti-SOX9 (1:200 dilution, Abcam), anti-HNF-4 α (1:250 dilution, Santa Cruz Biotechnology), anti-albumin (1:100 dilution, Abcam), anti-MRP2 (1:250 dilution, Abcam), anti-CYP3A4 (1:100 dilution, Santa Cruz Biotechnology), anti-CK18 (1:100 dilution, Abcam), and anti- α -SMA (1:100 dilution, Abcam) antibodies overnight at 4°C , followed by incubation with anti-mouse Alexa 488 (1:500 dilution, Invitrogen), anti-rabbit Alexa 488 (1:500 dilution, Invitrogen), anti-rabbit Alexa 594 (1:250 dilution, Invitrogen), anti-goat Alexa 594 (1:250 dilution, Invitrogen)-conjugated antibodies for 1 hour. Nuclei were co-stained with Hoechst 33342 (1:1,000 dilution, Molecular Probes). Fluorescent images were captured using an LSM900 laser scanning microscope (Zeiss).

Flow cytometry analysis

Exosome-specific markers (CD9, CD63, and CD81) and non-exosomal markers (GM130 and calnexin) were quantified

using flow cytometry. For flow cytometry analysis, 1×10^9 particles of exosomes and CD9 magnetic beads (Invitrogen) were incubated overnight at 4 °C. After the washing step, CD9-PE (BD Biosciences), CD63-PE (BD Biosciences), CD81-APC (BD Biosciences), GM130-PE (Santa Cruz Biotechnology), and calnexin-FITC (Santa Cruz Biotechnology) were reacted as secondary antibodies. After labeling with the antibodies, the samples were quantified using a flow cytometer (FACSCantoII, BD Biosciences).

Furthermore, flow cytometry analysis was carried out to investigate the uptake of exosomes by HHStEC. Briefly, HHStEC were seeded at 1×10^5 cells/well onto a 6-well plate and incubated at 37 °C and 5% CO₂ overnight for the confluence. Then, the cells were treated with 50 µg of DiR-labeled exosomes per well and incubated for 6 hours at 37 °C. Cells were measured by flow cytometry at the wavelength of 638 nm (APC-A750 channel).

In vivo biodistribution and fluorescence optical imaging

C57BL/6 mice were randomly divided into 3 groups: control (PBS), BMMSCs-derived exosomes (BMMSCs-exo), and hCdHs-derived exosomes (hCdHs-exo). Mice were injected through the tail vein with 200 µL of PBS, DiR-labeled BMMSCs-exo or DiR-labeled hCdHs-exo. The distribution of fluorescence in organs was examined with a VISQUE InVivo Smart-LF imaging system (Vieworks). Mice were anesthetized at 1, 2, or 3 hours after injections, and images were obtained at each time point. The optical density of fluorescent dye *in vivo* was determined at the excitation and emission wavelengths of 747 nm and 774 nm, respectively.

Experimental animal models

All animals were housed for 1 week before the experiment for proper acclimatization in a well-ventilated room with adjusted temperature and humidity under a 12-hour light/12-hour dark cycle.

C57BL/6 mice (7–9 weeks old, male, $n = 18$) were randomly divided into normal ($n = 3$) and experimental ($n = 15$) groups. The mice in the experimental group were further divided into 5 subgroups: oil, carbon tetrachloride (CCl₄), PBS, BMMSCs-exo, and hCdHs-exo. CCl₄ and exosomes were administered as described in the experimental scheme. The CCl₄, PBS, BMMSCs-exo, and hCdHs-exo groups ($n = 12$) were intraperitoneally administered CCl₄ (Sigma) with olive oil (1:1, v/v, 2 µL/g body weight) twice to induce liver damage. The oil group ($n = 3$) received the same volume of oil and was used as a control. Tail vein injections were then used to administer BMMSCs-exo or hCdHs-exo (4×10^7 particles in 200 µL of PBS) to the BMMSCs-exo and hCdHs-exo groups ($n = 3$ each), respectively, 3 times at 24-hour intervals. The PBS group ($n = 3$) was given only 200

µL of PBS. Mice were sacrificed 2 days after the last exosome injection. The livers and blood samples were collected and subjected to histologic and biochemical analyses.

Biochemical analysis

Serum levels of ALT and AST in exosome-treated and control mice were assessed using an automated chemistry analyzer (Fujifilm) according to the manufacturer's instructions.

Histological analysis

The harvested livers were immediately fixed with 4% PFA, embedded in paraffin, sectioned at 3 µm thickness, and deparaffinized. Deparaffinized sections were stained with H&E, and Masson's trichrome and Sirius red, according to standard protocols for analysis of histologic structure and fibrotic areas, respectively. Liver fibrosis was quantified by measuring collagenous fibrotic areas stained in red (Sirius red sections) and blue (Masson's trichrome sections) in 3 random fields per section from images, using multiphase image analyses with ImageJ software.

The degree of hepatic fibrosis was assessed using the Ishak modified scoring system [24]. The Ishak scoring criterion ranges from 0 (no fibrosis) to 6 (cirrhosis): mild fibrosis (Ishak, 0–2) to severe fibrosis (Ishak, 3–6).

Immunohistochemistry

Liver sections were deparaffinized and rehydrated in a descending alcohol series. Heat-induced target antigen retrieval was performed on the deparaffinized sections, and the sections were treated with 0.3% H₂O₂ solution (Sigma) at room temperature for 30 minutes to block the endogenous peroxidase. After washing, the sections were incubated with primary antibody, anti- α -SMA (1:100 dilution, Abcam) at 4 °C for 24 hours. Then the sections were incubated with horseradish-peroxidase-conjugated secondary antibody (DAKO), and the bound antibody was visualized as a brown precipitate with 3,3'-diaminobenzidine chromogen (DAKO). Lastly, the sections were counterstained with hematoxylin at room temperature for 5 minutes. Randomly captured images from 3 independent liver sections were examined to quantify the fibrosis area. All images were acquired using a light microscope (Nikon).

Statistical analyses

Statistical analyses were performed using GraphPad Prism 13.0 (GraphPad Software). The data are represented as the mean \pm standard error of the mean. The P-values were calculated using the t-test and 1-way analysis of variance to compare 2 or more groups. Based on the level of statistical significance, results are categorized as follows: *P < 0.05, **P < 0.01, ***P < 0.001, ****P < 0.0001, and not significant (P \geq 0.05).

RESULTS

Isolation and characterization of exosomes derived from human chemically derived hepatic progenitors and bone marrow mesenchymal stem cells

We used a perfusion method to isolate human primary hepatocytes (hPHs) from liver tissue [20]. Isolated hPHs were

cultured in a reprogramming medium containing a specific set of small molecules, including HGF, A83-01, and CHIR99021 (collectively referred to as HAC), as previously described by Kim et al. [20] To assess whether hCdHs cultured in HAC medium transitioned from hepatocytes to hepatic progenitors, we analyzed the RNA expression levels of hepatic progenitors (*CK19*, *EpCAM*, *SOX9*, and *CD44*) and hepatocyte (*CK18*, *ALB*, *HNF4 α* , *CYP1A2*, *ASGR1*, and *MRP2*) markers in both hCdHs and hPHs

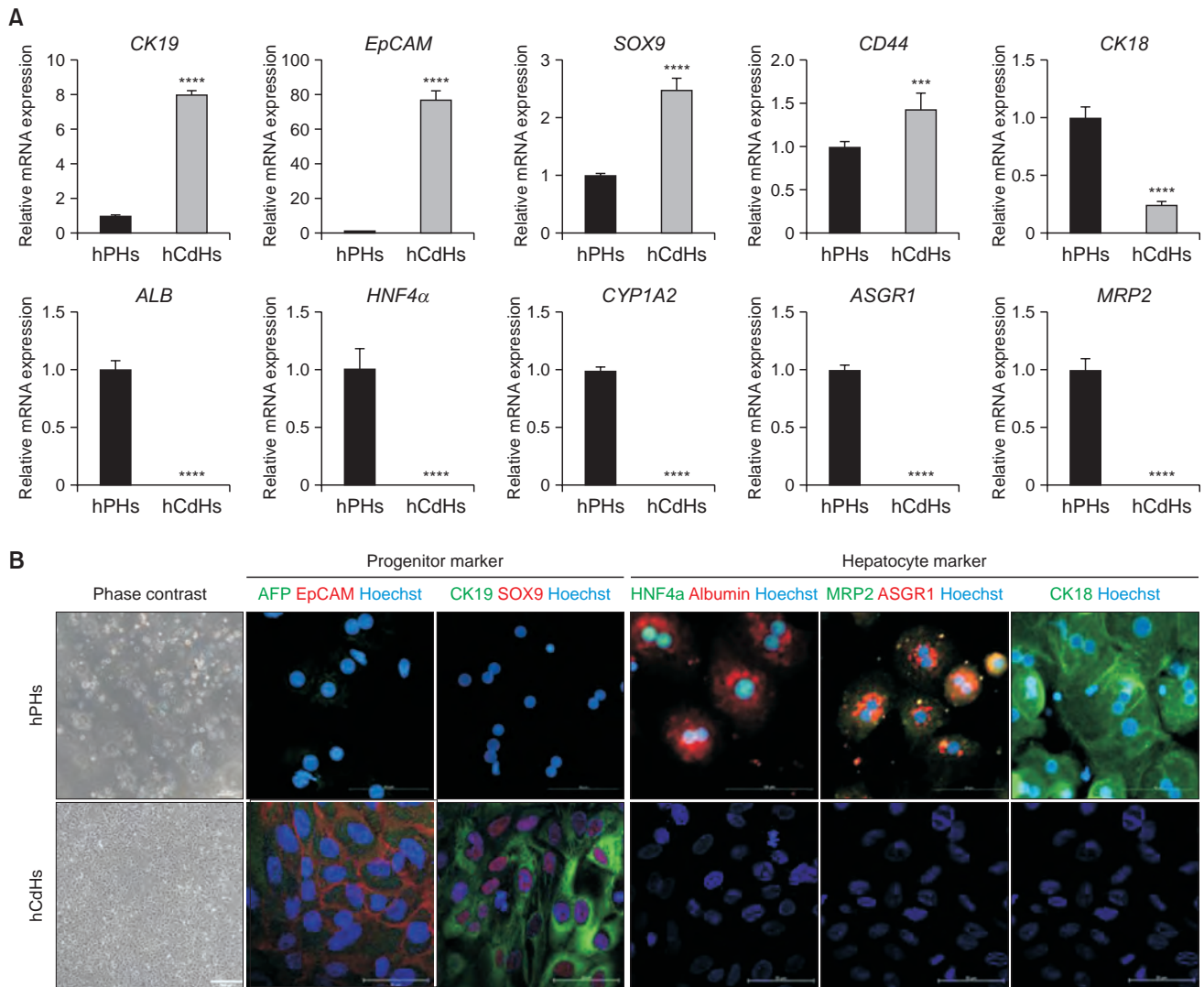


Fig. 1. Isolation and characterization of exosomes derived from human chemically derived hepatic progenitors (hCdHs) and bone marrow mesenchymal stem cells (BMMSCs). (A) Quantitative real-time PCR analysis of hepatic progenitor marker (*CK19*, *EpCAM*, *SOX9*, and *CD44*) and hepatocyte marker (*CK18*, *ALB*, *HNF4 α* , *CYP1A2*, *ASGR1*, and *MRP2*) genes. *GAPDH* was used as an internal control. Data are shown as mean \pm standard deviation ($n = 3$). Data were analyzed by 2-tailed t-tests (*** $P < 0.001$, **** $P < 0.0001$). (B) Representative phase contrast (left) and double immunofluorescence (right) images of staining for the hepatic progenitor markers AFP (green)/EpCAM (red) and CK19 (green)/SOX9 (red), and for the hepatocyte markers HNF4 α (green)/albumin (red), MRP2 (green)/ASGR1 (red), and CK18 (green). Nuclei were counterstained with Hoechst 33342 (blue). Scale bars, 500 μm and 100 μm . (C) Brightfield imaging of hCdHs and BMMSCs. Scale bars, 500 μm . (D) Size distribution of hCdHs-derived exosomes (hCdHs-exo) and BMMSCs-derived exosomes (BMMSCs-exo) as assessed by nanoparticle tracking analysis. (E) Morphological analysis of isolated hCdHs-exo and BMMSCs-exo by cryogenic transmission electron microscopy (white arrows). Scale bar, 200 nm. (F) Expression of exosomal (CD9, CD63, and CD81) and non-exosomal (GM130 and calnexin) markers was evaluated in isolated exosome samples by flow cytometry using marker-specific antibodies. (G) Expression of exosome markers in cell lysates and exosomes were confirmed by western blotting. *GAPDH*, glyceraldehyde-3-phosphate dehydrogenase.

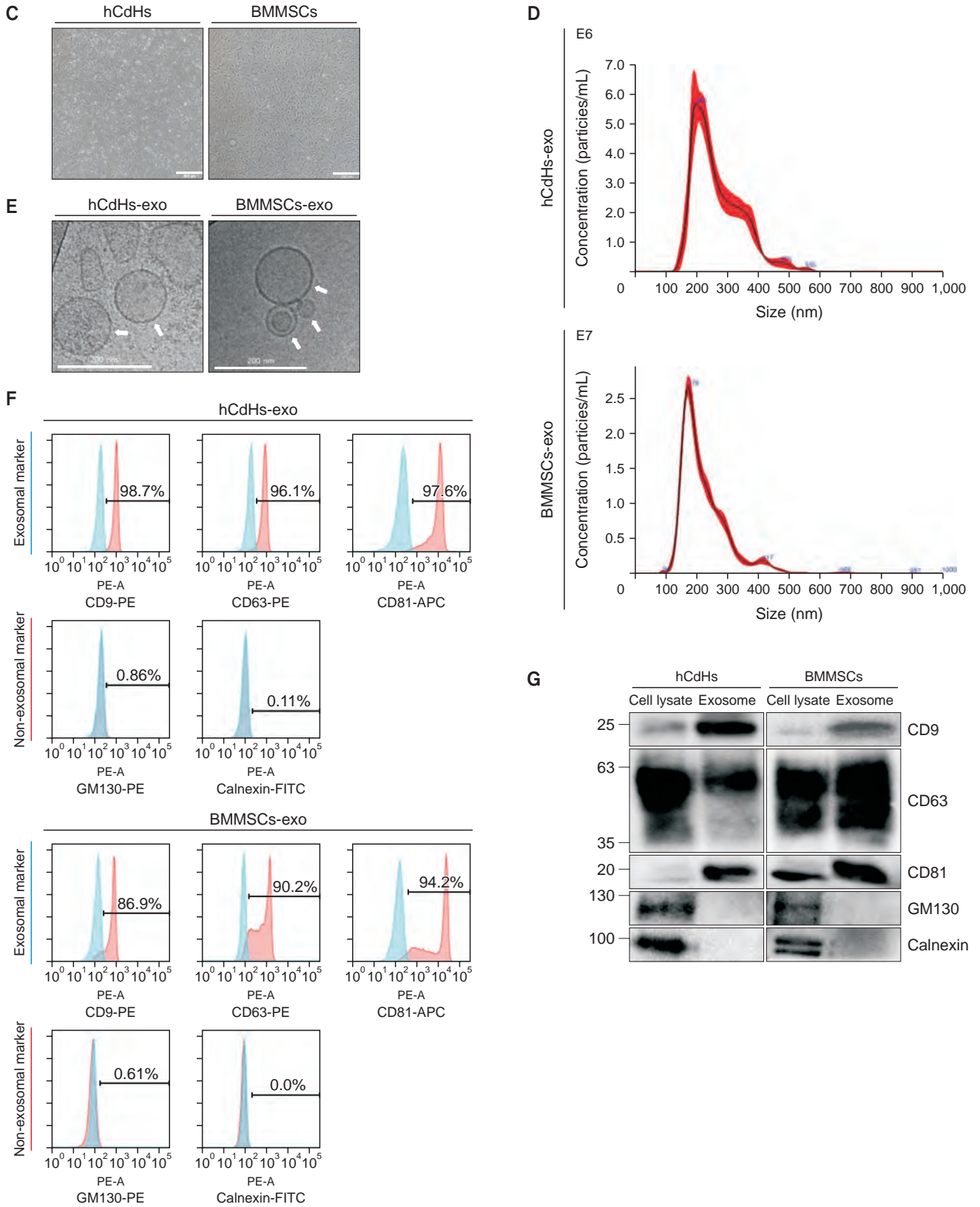


Fig. 1. Continued.

(Fig. 1A). Additionally, the protein expression levels of these hepatic progenitor and hepatocyte markers were confirmed using immunofluorescence staining (IF) analysis (Fig. 1B). It was confirmed that hepatocyte markers exhibited higher expression in hPH and hepatic progenitor markers were more expressed in hCdHs. These results indicate that hCdHs cultured in HAC medium indeed transitioned from hepatocytes to hepatic progenitors.

Following the successful generation of hCdHs, exosomes were isolated from hCdHs and BMMSCs by culturing cells in bulk (Fig. 1C) and subjecting the culture medium to ultracentrifugation. To confirm the isolation and purity of exosomes, we analyzed the properties of exosomes. The size distribution and concentration of the exosomes were evaluated by NTA (Fig. 1D). The size of the isolated exosomes corresponded to the known average size of exosomes (50–200 nm). Cryo-TEM allowed for the identification of double lipid bilayer structures of exosomes, and, in rare cases, smaller exosomes contained within larger ones were observed (Fig. 1E). Flow cytometry analysis was conducted using exosome-specific markers. Compared with the control beads, hCdHs-exo showed a shift rate of at least 96% in the exosomal markers (CD9, CD63, and CD81), while BMMSCs-exo showed a shift rate of at least 86%. Conversely, both types of exosomes showed a shift rate of less than 1% in the non-exosomal markers (GM130 and calnexin) (Fig. 1F). Additionally, western blot analysis was performed for the markers used in flow cytometry. Specific bands were observed for the exosomal

markers (CD9, CD63, and CD81) in the exosome samples, while the non-exosomal markers (GM130 and calnexin) were only present in the cell lysates (Fig. 1G). These results suggest that we successfully isolated exosomes from hCdHs and BMMSCs.

Human chemically derived hepatic progenitors-derived exosomes suppress hepatic stellate cell activation by transforming growth factor beta 1

Hepatic stellate cells (HSCs) are a key fibrogenic cell type that contributes to liver fibrosis. Liver fibrogenesis is initiated by HSC activation. Upon liver injury, HSCs become activated and proliferative and produce extracellular matrix (ECM), such as collagens, in the damaged liver. Excessive accumulation of ECM perturbs the normal function of the liver and eventually leads to damage of the liver. Hence, regulating HSC activation could be a potential therapeutic strategy for liver damage [25]. Therefore, in order to confirm the effect of isolated exosomes on alleviating liver damage, we treated exosomes with activated HSCs. Initially, to confirm the efficient uptake of exosomes by HSCs, previously isolated exosomes were stained with DiR, a lipid membrane dye emitting red fluorescence, and then administered to HHStCs. DiR-stained exosomes were readily absorbed by HHStCs (Fig. 2A). Further, following the administration of stained exosomes to HHStCs, the degree of exosomal fluorescence expression within the cells was measured by flow cytometry analysis. This analysis showed that about 70% of the treated HHStCs exhibited fluorescence

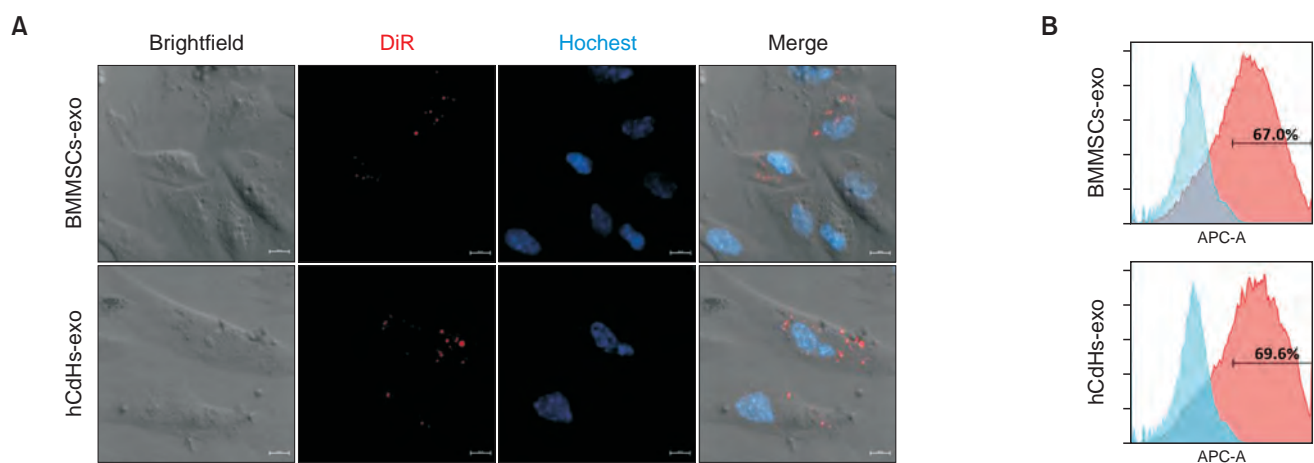


Fig. 2. Human chemically derived hepatic progenitors-derived exosomes (hCdHs-exo) suppress hepatic stellate cell activation by transforming growth factor beta 1 (TGF- β 1). (A) Confocal microscopy data were acquired after processing DiR-labeled exosomes in human hepatic stellate cells (HHStCs). Scale bars, 10 μ m. (B) Flow cytometry analysis of HHStC treated with DiR-labeled exosomes. (C) Representative phase contrast images of HHStCs treated with bone marrow mesenchymal stem cells-derived exosomes (BMMSCs-exo) or hCdHs-exo for 48 hours in the presence of TGF- β 1 (2 ng/mL). Scale bars, 100 μ m. (D) Western blot analysis of HHStC incubated with BMMSCs-exo or hCdHs-exo for 48 hours in the presence of TGF- β 1 (2 ng/mL). (E) Representative immunofluorescence images of alpha smooth muscle actin (α -SMA; green). Nuclei were counterstained with Hoechst 33342 (blue). Scale bars, 100 μ m. (F) Quantitative real-time PCR analysis of liver fibrosis marker genes (α -SMA, *Col1 α 1*, *TGF β 1*, and *TIMP1*). *GAPDH* was used as an internal control. Data are shown as the mean \pm standard error of mean (n = 3 independent experiments). Data were analyzed by 2-tailed t-tests (*P < 0.05, ***P < 0.001, and ****P < 0.0001). NS, not significant.

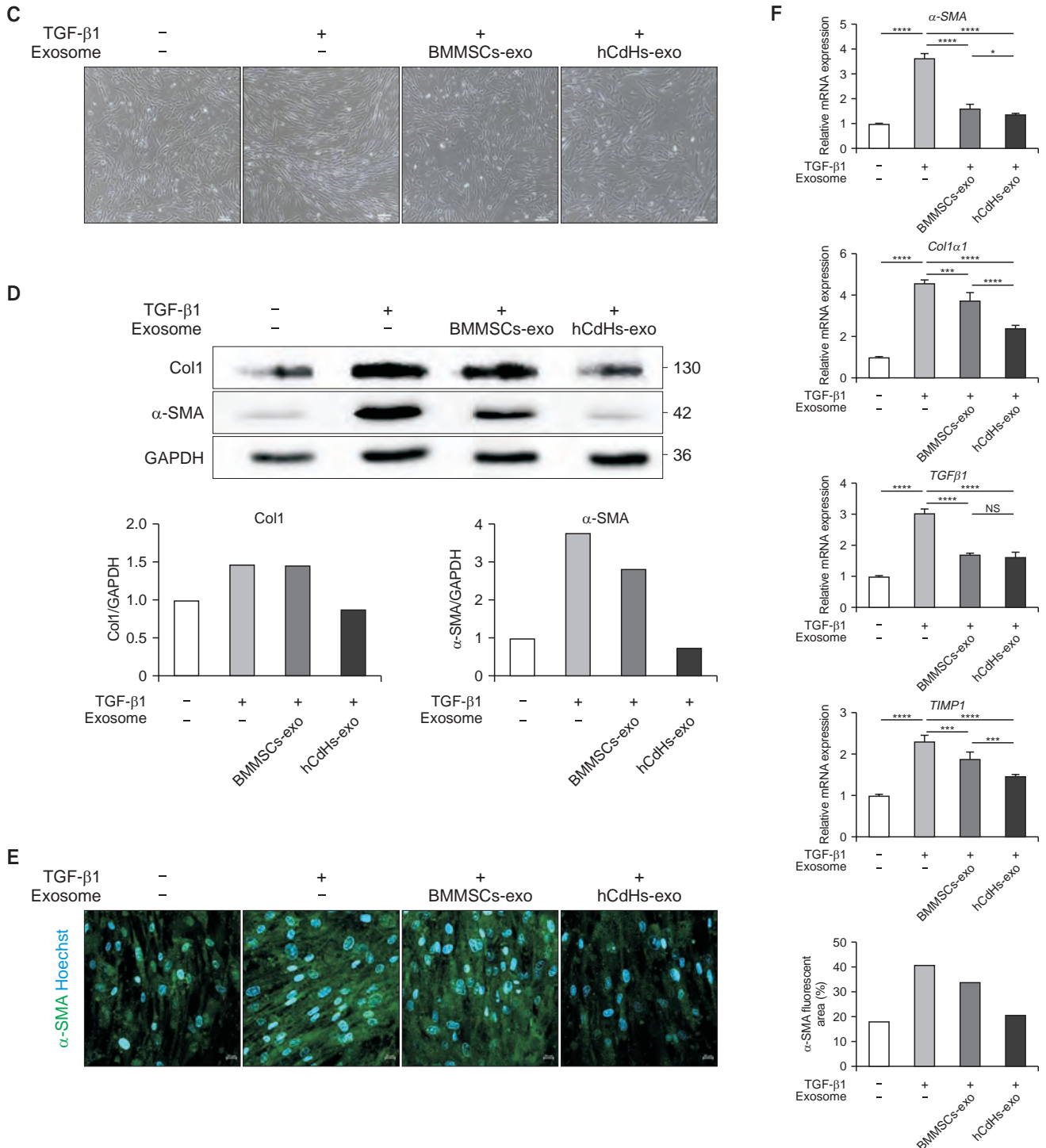


Fig. 2. Continued.

from the exosomes (Fig. 2B), suggesting that the 2 types of exosomes were efficiently absorbed by the HSCs intended for future experiments.

Subsequently, we determined whether hCdHs-exo and BMMSCs-exo might inhibit the activation of HSCs, induced by TGF-β1. After 48 hours, microscopic observation revealed that

the fibrotic morphological changes in HHStECs were reduced by the exosome treatment (Fig. 2C). After harvesting the cells, western blot analysis was conducted to confirm the protein expression of α-SMA and collagen type I (Col1), markers of liver fibrosis and HSC activation, respectively (Fig. 2D). HHStECs were successfully activated by TGF-β1, and the treatment with

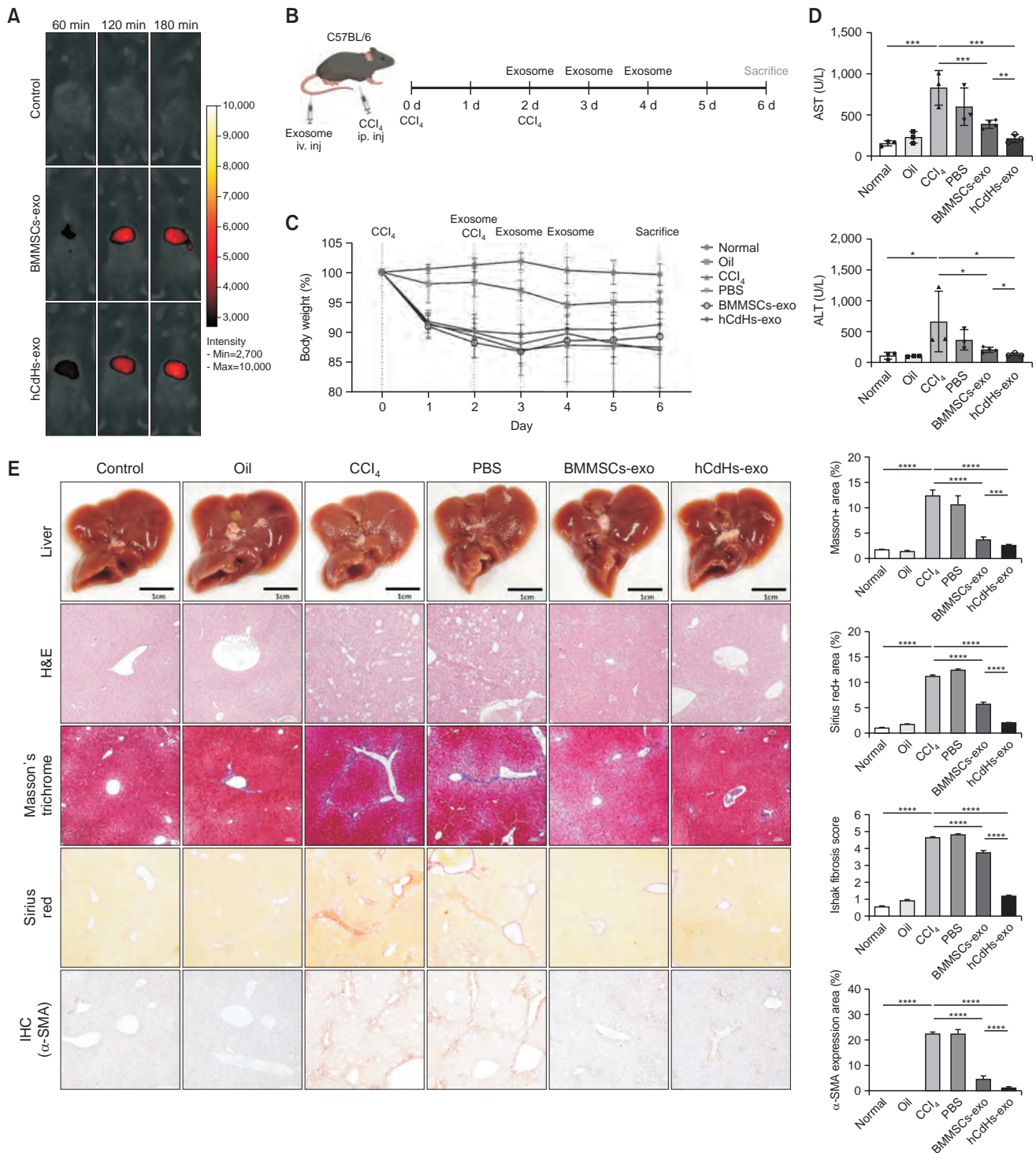


Fig. 3. Human chemically derived hepatic progenitors-derived exosomes (hCdHs-exo) alleviate liver damage induced by carbon tetrachloride (CCl₄). (A) 1, 2, and 3 hours after tail vein injection of DiR-labeled bone marrow mesenchymal stem cells-derived exosomes (BMMSCs-exo) and hCdHs-exo, *in vivo* tracking was confirmed using an *in vivo* smart imaging system. (B) Diagram of the experimental plan. (C) Body weight changes during treatment with CCl₄ via intraperitoneal injection and with phosphate-buffered saline (PBS), BMMSCs-exo, and hCdHs-exo via tail vein injection. (D) ALT and AST levels analyzed by collecting blood from sacrificed mice. Each value is the mean \pm standard error of mean (SEM) (n = 3 independent experiments). (E) Representative photographs of livers from mice in each group. Histopathologic features of liver sections from animals with CCl₄-induced liver damage were evaluated using H&E, Masson's trichrome, Sirius red, and immunohistochemistry staining (IHC; alpha smooth muscle actin [α -SMA]). Scale bars, 100 μ m. Liver histopathology grading was evaluated by an Ishak (modified Knodell) scoring system after treatment. Data are expressed as the mean \pm SEM (n = 3–5; *P < 0.05, **P < 0.01, ***P < 0.001, and ****P < 0.0001). NS, not significant.

exosomes effectively suppressed the activation. IF analysis using an α -SMA antibody was performed to verify the level of protein expression (Fig. 2E). In addition, the RNA expression levels of fibrosis markers as α -SMA, Col1 alpha 1 (*Col1 α 1*), *TGF- β 1*, and TIMP metalloproteinase inhibitor 1 (*TIMP1*) effectively suppressed the activation of HHStCs by exosome treatment (Fig. 2F). Interestingly, the ability of hCdHs-exo to suppress HSC activation was superior to that of BMMSCs-exo. These findings suggest that hCdHs-exo could be effective in inhibiting the activation of HSCs involved in liver fibrosis.

Human chemically derived hepatic progenitors-derived exosomes alleviate liver damage induced by CCl₄

In this study, to compare the effect of exosomes in alleviating liver damage *in vivo*, C57BL/6 mice were used to induce liver damage using CCl₄.

Initially, to verify whether exosomes could effectively migrate to and be absorbed by the liver, DiR-stained exosomes were intravenously injected into mice, and fluorescence expression in the liver was observed using an *in vivo* imaging system. Both types of exosomes were efficiently transported to and absorbed by the liver (Fig. 3A).

Subsequently, following the schematic, CCl₄ was administered twice to cause liver damage in mice, and then exosomes were injected once a day for 3 days to confirm the degree to which liver damage was alleviated (Fig. 3B). Liver damage induced by CCl₄ was confirmed by a decrease in mouse weight (Fig. 3C). In addition, AST and ALT levels, which are indicators of liver damage confirmed through blood biochemical analysis, were increased by CCl₄, but were recovered by the administration of hCdHs-exo and BMMSCs-exo (Fig. 3D). Moreover, we further assessed the extent of liver damage through histological analysis. Hepatocyte destruction increased by CCl₄, confirmed through H&E staining, was recovered by administration of exosomes. Furthermore, it was confirmed that the increase in collagen fibers confirmed through Masson's trichrome staining and Sirius red staining and the increase in α -SMA, a liver fibrosis marker protein confirmed through immunohistochemistry, were alleviated by injecting exosomes. The results of tissue staining and the corresponding quantified data also confirmed that exosome treatment had a significant effect on the recovery from liver damage (Fig. 3E). Moreover, hCdHs-exo demonstrated superior efficacy in alleviating liver damage compared with that of BMMSCs-exo. These findings indicate that hCdHs-exo is effective against CCl₄-induced liver injury in C57BL/6 mice, showing superior therapeutic efficacy compared to BMMSCs-exo.

DISCUSSION

Our results show that hCdHs can be successfully generated using a HAC reprogramming medium. The transformation of these cells from hepatocyte to hepatic progenitor characteristics was confirmed by RNA and protein expression analyses. This finding suggests that the production and use of hCdHs, which are capable of proliferating through hepatocytes, may play an important role in the regeneration and repair process of liver cells. Furthermore, we confirmed the identity of vesicles isolated from hCdHs and BMMSCs as exosomes through analyses of their size, shape, and protein markers. Notably, the expression of exosomal markers (CD9, CD63, and CD81), which are tetraspanin markers, served as a crucial indicator of exosome identity. This means that exosomes were released not only from BMMSCs but also from hCdHs, and that exosomes were successfully isolated from both cells.

Liver fibrosis, a representative type of liver damage, primarily progresses through the production of α -SMA and Col1 by activated HSCs [26]. Therefore, inhibiting activated HSCs may suppress liver damage. hCdHs-exo inhibited TGF- β 1-induced activation of HSCs by reducing protein and RNA expression of fibrosis markers (α -SMA, Col1). Additionally, the ability of hCdHs-exo to inhibit HSCs activation was better than that of BMMSCs-exo. This indicates that hCdHs-exo is effective in suppressing HSCs activation by TGF- β 1 and has a superior inhibitory ability than BMMSCs-exo.

Injecting hCdHs-exo into a mouse model with CCl₄-induced liver damage decreased liver damage indicators and promoted tissue repair. Specifically, the exosome treatment lowered the AST and ALT levels, reduced liver cell destruction and the collagen fiber increase, and decreased α -SMA protein expression. The alleviation of liver damage by hCdHs-exo is likely attributable to the promotion of liver tissue recovery by various growth factors and proteins contained within the exosomes. Additionally, compared with BMMSCs-exo, hCdHs-exo demonstrated a superior liver damage alleviation effect under certain conditions and may therefore be a promising candidate for the treatment of liver fibrosis. These findings suggest that hCdHs-exo could represent a novel therapeutic strategy for liver diseases.

The findings of this study demonstrate the potential of hCdHs and hCdHs-exo as effective therapeutic agents for the treatment of liver damage and fibrosis. Moreover, our study emphasizes the potential advantage of exosome-based therapy methods, which can utilize the regenerative and tissue repair capabilities of stem cells while minimizing the side effects associated with stem cell transplantation. Specifically, the use of exosomes isolated from autologous cells can reduce the risk of transplant rejection and other transplantation-related issues and significantly decrease the risk of side effects such as cancer

due to uncontrolled proliferation and differentiation.

The study's limitations include a need for further research aimed at improving the yield and safety of exosomes, as well as better characterizing the internal contents of exosomes derived from hCdHs. Exosomes show a much lower yield compared to the materials used, and various studies are underway to address this issue. Additionally, efficacy evaluation in various types of liver disease models and validation through large-scale clinical trials are necessary. Further research is also needed to analyze the contents of hCdHs-exo to understand which proteins and genes are involved in alleviating liver damage and how they are associated with specific pathways or mechanisms.

In conclusion, this study demonstrates the effectiveness of exosomes derived from hCdHs in alleviating liver damage, providing a novel approach and opening new possibilities for the treatment of liver disease. Through further research exploring the efficacy and safety of hepatic progenitor exosomes, significant progress can be made in the field of liver disease treatment.

SUPPLEMENTARY MATERIALS

Supplementary Tables 1 and 2 can be found via <https://doi.org/10.4174/astr.2024.107.5.252>.

ACKNOWLEDGEMENTS

Hanyang University Medical Center provided human liver

tissues.

Fund/Grant Support

This work was supported by the National Research Foundation of Korea (2022R1A2C2004593 and 2023R1A2C1005279). This work was also supported by the Korean Fund for Regenerative Medicine funded by the Ministry of Science and ICT, and the Ministry of Health and Welfare (21A0401L1).

Conflict of Interest

No potential conflict of interest relevant to this article was reported.

ORCID iD

Min Kim: <https://orcid.org/0000-0002-7754-5311>

Tae Hun Kim: <https://orcid.org/0000-0002-0638-9649>

Elsy Soraya Silva Salas: <https://orcid.org/0000-0002-3897-018X>

Soyoung Jeon: <https://orcid.org/0009-0008-5470-4325>

Ji Hyun Shin: <https://orcid.org/0000-0002-1897-7990>

Dongho Choi: <https://orcid.org/0000-0002-1255-1964>

Author's Contributions

Conceptualization: MK, JHS, DC

Formal Analysis, Methodology: MK, JHS, DC

Investigation: MK, THK, ESSS, SJ

Writing – Original Draft: MK, JHS, DC

Writing – Review & Editing: All authors

REFERENCES

- Théry C, Zitvogel L, Amigorena S. Exosomes: composition, biogenesis and function. *Nat Rev Immunol* 2002;2:569-79.
- van der Pol E, Böing AN, Harrison P, Sturk A, Nieuwland R. Classification, functions, and clinical relevance of extracellular vesicles. *Pharmacol Rev* 2012;64:676-705.
- Théry C. Exosomes: secreted vesicles and intercellular communications. *F1000 Biol Rep* 2011;3:15.
- Kalluri R. The biology and function of exosomes in cancer. *J Clin Invest* 2016;126:1208-15.
- Nazimek K, Bryniarski K, Santocki M, Ptak W. Exosomes as mediators of intercellular communication: clinical implications. *Pol Arch Med Wewn* 2015;125:370-80.
- Aheget H, Mazini L, Martin F, Belqat B, Marchal JA, Benabdellah K. Exosomes: their role in pathogenesis, diagnosis and treatment of diseases. *Cancers (Basel)* 2020;13:84.
- Vlassov AV, Magdaleno S, Setterquist R, Conrad R. Exosomes: current knowledge of their composition, biological functions, and diagnostic and therapeutic potentials. *Biochim Biophys Acta* 2012;1820:940-8.
- Gutierrez-Millan C, Calvo Díaz C, Lanao JM, Colino CI. Advances in exosomes-based drug delivery systems. *Macromol Biosci* 2021;21:e2000269.
- Joo HS, Suh JH, Lee HJ, Bang ES, Lee JM. Current knowledge and future perspectives on mesenchymal stem cell-derived exosomes as a new therapeutic agent. *Int J Mol Sci* 2020;21:727.
- Mahla RS. Stem cells applications in regenerative medicine and disease therapeutics. *Int J Cell Biol* 2016;2016:6940283.
- Fox IJ, Daley GQ, Goldman SA, Huard J, Kamp TJ, Trucco M. Stem cell therapy: use of differentiated pluripotent stem cells as replacement therapy for treating disease. *Science* 2014;345:1247391.
- Trounson A, McDonald C. Stem cell therapies in clinical trials: progress and challenges. *Cell Stem Cell* 2015;17:11-22.
- Balistreri CR, De Falco E, Bordin A, Maslova O, Koliada A, Vaiserman A. Stem

- cell therapy: old challenges and new solutions. *Mol Biol Rep* 2020;47:3117-31.
14. Nikfarjam S, Rezaie J, Zolbanin NM, Jafari R. Mesenchymal stem cell derived-exosomes: a modern approach in translational medicine. *J Transl Med* 2020;18:449.
 15. Yu B, Zhang X, Li X. Exosomes derived from mesenchymal stem cells. *Int J Mol Sci* 2014;15:4142-57.
 16. Hade MD, Suire CN, Suo Z. Mesenchymal stem cell-derived exosomes: applications in regenerative medicine. *Cells* 2021;10:1959.
 17. Gołębiewska JE, Wardowska A, Pietrowska M, Wojakowska A, Dębska-Ślizień A. Small extracellular vesicles in transplant rejection. *Cells* 2021;10:2989.
 18. Lou G, Chen Z, Zheng M, Liu Y. Mesenchymal stem cell-derived exosomes as a new therapeutic strategy for liver diseases. *Exp Mol Med* 2017;49:e346.
 19. Maqsood M, Kang M, Wu X, Chen J, Teng L, Qiu L. Adult mesenchymal stem cells and their exosomes: sources, characteristics, and application in regenerative medicine. *Life Sci* 2020;256:118002.
 20. Kim Y, Kang K, Lee SB, Seo D, Yoon S, Kim SJ, et al. Small molecule-mediated reprogramming of human hepatocytes into bipotent progenitor cells. *J Hepatol* 2019;70:97-107.
 21. Salas-Silva S, Kim Y, Kim TH, Kim M, Seo D, Choi J, et al. Human chemically-derived hepatic progenitors (hCdHs) as a source of liver organoid generation: application in regenerative medicine, disease modeling, and toxicology testing. *Biomaterials* 2023;303:122360.
 22. Kim Y, Kim YW, Lee SB, Kang K, Yoon S, Choi D, et al. Hepatic patch by stacking patient-specific liver progenitor cell sheets formed on multiscale electrospun fibers promotes regenerative therapy for liver injury. *Biomaterials* 2021;274:120899.
 23. Kim M, Kim Y, Silva ES, Adisasmita M, Kim KS, Jung YK, et al. Enhancing generation efficiency of liver organoids in a collagen scaffold using human chemically derived hepatic progenitors. *Ann Hepatobiliary Pancreat Surg* 2023;27:342-9.
 24. Ishak K, Baptista A, Bianchi L, Callea F, De Groote J, Gudat F, et al. Histological grading and staging of chronic hepatitis. *J Hepatol* 1995;22:696-9.
 25. Kim J, Lee C, Shin Y, Wang S, Han J, Kim M, et al. sEVs from tonsil-derived mesenchymal stromal cells alleviate activation of hepatic stellate cells and liver fibrosis through miR-486-5p. *Mol Ther* 2021;29:1471-86.
 26. Campana L, Iredale JP. Regression of liver fibrosis. *Semin Liver Dis* 2017;37:1-10.